The radiative return and form factors at large Q^2

J.H. Kühn [a] *

[a]Institut für Theoretische Teilchenphysik, Universität Karlsruhe,
D-76128 Karlsruhe, Germany.

The measurement of the pion form factor and, more generally, of the cross section for electron–positron annihilation into hadrons through the radiative return has become an important task for high luminosity colliders such as the Φ- or B-meson factories. For a detailed understanding and analysis of this reaction, the construction of a Monte Carlo program, PHOKHARA, has been undertaken. A brief overview of the most recent developments is presented, which include the combination of initial- and final-state radiation in the case of two-pion production. Baryon pair production is now included and the pion form factor is extended into the region of large Q^2. A model for the kaon form factor is discussed which is fitted to K^+K^- and $K^0\bar{K}^0$ data and which leads to predictions for the τ-decay into $K^-K^0\nu$.

1. Introduction

Electron–positron annihilation into hadrons is one of the basic reactions of particle physics, crucial for the understanding of hadronic interactions [1]. The recent advent of Φ- and B-meson factories with their enormous luminosities allows us to exploit the radiative return to explore the whole energy region from threshold up to the nominal energy of the collider. Photon radiation from the initial state reduces the cross section by a factor $\mathcal{O}(\alpha/\pi)$. However, this is easily compensated by the enormous luminosity of 'factories' and the advantage of performing the measurement over a wide range of energies in one homogeneous data sample [2] (for an early proposal along these lines, see [3]). In principle the reaction $e^+e^- \to \gamma +$ hadrons receives contributions from both initial- and final-state radiation. Only the former is of interest for the radiative return; the latter has to be eliminated by suitably chosen cuts. The proper analysis thus requires the construction of Monte Carlo event generators. The event generator EVA was based on a leading order treatment of ISR and FSR, supplemented by an approximate inclusion of additional collinear radiation based on structure functions and included two-pion [2] and four-pion final states [4]. Subsequently the event generator PHOKHARA was developed; it is based on a complete next-to-leading order (NLO) treatment of ISR [5–8]. In its version 2.0 it included ISR at NLO and FSR at leading order (LO) for $\pi^+\pi^-$ and $\mu^+\mu^-$ final states and four-pion final states without FSR. A version which also includes $K\bar{K}$ and three-pion final states is currently inder construction [9].

Recent preliminary experimental results indeed demonstrate the power of the method and seem to indicate that a precision of one per cent or better is within reach [10]. In view of this progress a further improvement of theoretical understanding and MC-programs is necessary. PHOKHARA version 3.0 [11] allows for the 'simultaneous' emission of one photon from the initial and one photon from the final state, requiring only one of them to be hard. This includes in particular the radiative return to $\pi^+\pi^-(\gamma)$ and thus allows the measurement of the (one-photon) inclusive $\pi^+\pi^-$ cross section.

2. Final state radiation in next-to-leading order

The issue of photon radiation from the final states is closely connected to the question of $\pi^+\pi^-(\gamma)$ contributions to a_μ. Soft photon emis-

*Work supported in part by BMBF under grant number 05HT9VKB0, and SFB-TR/9.

sion is clearly described by the point-like pion model. Hard photon emission, with $E_\gamma \geq \mathcal{O}(100$ MeV), however, might be sensitive to unknown hadronic physics. Therefore the size of virtual, soft and hard corrections has to be studied separately. In [11] it has been argued that contributions from the hard region, above 100 MeV, are small with respect to the present experimental and theory-induced uncertainty.

Let us start with the process in leading order:

$$e^+ \ e^- \to \pi^+(p^+) \ \pi^-(p^-) \ \gamma \ . \tag{1}$$

The amplitude of interest describes radiation from the initial state (ISR). It is proportional to the pion form factor, evaluated at $Q^2 = (p^+ + p^-)^2$. However, radiation from the charged pions (FSR) evidently leads to the same final state and must be suppressed and controlled with sufficient precision. A variety of methods are described in more detail in [2,6,8,11].

The fully differential cross section describing photon emission can be split into three pieces

$$d\sigma = d\sigma_{\rm ISR} + d\sigma_{\rm FSR} + d\sigma_{\rm INT} \ , \tag{2}$$

which originate from the squared ISR and FSR amplitudes respectively, plus the interference term. Let us summarise the main points of the 'leading order' discussion [11]:

1. The cross sections for photon emission from ISR and FSR can be disentangled as a consequence of the marked difference in angular distributions between the two processes. This observation is completely general and does not rely on any model like sQED for FSR. This allows us to measure the cross section for $\sigma(e^+e^- \to \gamma^* \to \pi^+\pi^-\gamma)$ directly for fixed s as a function of E_γ, an important ingredient in the analysis of hadronic contributions to a_μ. Alternatively we can employ suitable angular cuts to separate the two components.

2. Various charge-asymmetric distributions can be used for independent tests of the FSR model amplitude, with the forward–backward asymmetry as simplest example. Typically the charge asymmetry is large in the region where ISR and FSR are comparable in size and small when the separation is clean and simple from general considerations. A typical case for this second possibility is the radiative return at $\sqrt{s} = 10.52$ GeV, at the B-meson factories, where the $\pi^+\pi^-\gamma$ final state is completely dominated by ISR.

Intuitively it should also be possible to exploit the radiative return for the extraction of FSR for arbitrary invariant mass $\sqrt{s'}$ of the $\pi^+\pi^-\gamma$ system through the reaction

$$e^+e^- \to \gamma\gamma^*(\to \pi^+\pi^-\gamma) \ . \tag{3}$$

The implementation of this two-step process has been achieved in PHOKHARA 3.0 and the impact of the new corrections on a few selected distributions has been discussed in [11]. Let us recall the meaning of various abbreviations: ISRNLO corresponds to the ISR cross section calculated at NLO without any FSR. IFSLO includes in addition FSR at LO. Finally, IFSNLO stands for ISR and FSR at NLO as implemented in the new version of PHOKHARA (version 3.0).

For a cms energy of 1.02 GeV, relevant for the KLOE experiment, the IFSNLO correction to the cross section is relatively big at low Q^2, if no cuts are applied. Below the ρ resonance, they grow from zero at the resonance to 10% of the IFSLO cross section near the production threshold, while they remain small above the ρ resonance. This is due to the fact that the ISR leading to the ρ meson is strongly enhanced. Subsequently the ρ decays into $\pi^+\pi^-\gamma$, with a large contribution from the region where Q^2, the invariant mass of the $\pi^+\pi^-$, is low. Of course this is smeared by the width of the ρ, but the above discussion remains valid and the contribution from the newly implemented diagrams, through the reaction $e^+e^- \to \gamma\rho(\to \gamma\pi^+\pi^-)$, is sizeable.

The standard KLOE cut on the track mass reduces FSR further, to less than 1% for most of the Q^2 range, apart of the high values of Q^2, where the corrections remain at the level of 2%-3% (Fig. 1, lower curve). The behaviour of the additional contribution at $\sqrt{s} = 10.52$ GeV is qualitatively similar.

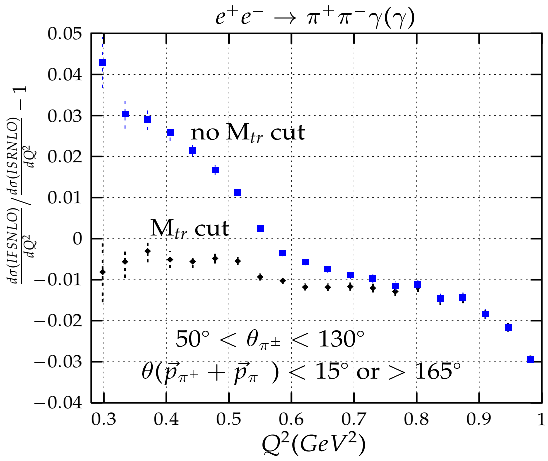

Figure 1. Comparison of the Q^2 differential cross sections for $\sqrt{s} = 1.02$ GeV. Cuts on the missing momentum direction and the track mass are imposed as discussed in the text.

3. Nucleon form factors at B-meson factories

The importance of measuring the nucleon form factor has been repeatedly emphasized in the literature (e.g. [12–14] and refs therein). Recent experiments at Jefferson Lab have explored the ratio of electric and magnetic form factors in the space-like region up to 5.6 GeV^2, using the recoil polarization method; their results show disagreement with data obtained with the Rosenbluth method. Data in the time-like region based on electron–positron annihilation into proton–antiproton, and the inverse reactions only extend to 6 GeV^2. These latter measurements exhibit fairly large errors and do not provide a separation of the contributions from the two form factors.

In [15] the potential of the radiative return at B-meson factories has been be explored. These measurements will cover the region from threshold up to 8 or even 9 GeV^2 with sufficient counting rates. Not surprisingly, many aspects of the radiative return are quite similar to those of the reaction $e^+e^- \to p\bar{p}$. In particular, it is again the square of the electric and magnetic form factors, which can be determined separately through the analysis of angular distributions.

Radiative corrections are indispensable for a precise interpretation of the data. Furthermore, given the limited acceptance and the asymmetric kinematic configuration at present B-meson factories, a Monte Carlo event generator is required to demonstrate the feasibility of the measurement. This has motivated the extension of the generator to a new version, PHOKHARA 4.0. In this case photon emission from the initial state only (ISR) was considered. Final-state radiation is small if the reaction is considered at a centre of mass (cms) collider energy of 10.5 GeV.

Cross sections and distributions for $e^+e^- \to N\bar{N}$ are conveniently expressed in terms of the electric and magnetic form factors G_M^N and G_E^N, where N stands for proton or neutron. The choice of form factors adopted in the program is described in detail in [15]. It is, however, set up in a modular form such that the two form factors can be easily modified and replaced by the user.

A qualitative discussion of form factor measurements through the radiative return, can be based on the leading order process

$$e^+(p_1) + e^-(p_2) \to \bar{N}(q_1) + N(q_2) + \gamma(k) \ . \quad (4)$$

From the simple analytical results it is straightforward to evaluate production rates, to understand the qualitative aspects of angular distributions, and to develop strategies for the separation of the electric and the magnetic form factor.

The differential cross section for reaction (4) (with ISR only) can be written as

$$d\sigma = \frac{1}{2s} L_{\mu\nu} H^{\mu\nu} \, d\Phi_2(p_1+p_2; Q, k) d\Phi_2(Q; q_1, q_2) \frac{dQ^2}{2\pi}, \quad (5)$$

where $L_{\mu\nu}$ and $H^{\mu\nu}$ are the leptonic and hadronic tensors respectively. For notation, definitions and an explicit form of the leptonic tensor, see for instance [4,7]. The hadronic tensor is given by

$$H_{\mu\nu} = 2|G_M^N|^2 (Q_\mu Q_\nu - g_{\mu\nu} Q^2) - \frac{8\tau}{\tau - 1} \left(|G_M^N|^2 - \frac{1}{\tau} |G_E^N|^2 \right) q_\mu q_\nu \ . \quad (6)$$

The nucleon and antinucleon momenta are denoted by q_1 and q_2 respectively. $Q = q_1 + q_2$, $\tau = Q^2/4m_N^2$ and $q = (q_2 - q_1)/2$.

Integrating over the whole range of nucleon angles and the photon azimuthal angle, and restricting the photon polar angle within $\frac{m_e}{\sqrt{s}} \ll \theta_\gamma^{\rm min} < \theta_\gamma < \pi - \theta_\gamma^{\rm min}$, the differential cross section factorizes into the cross section for electron–positron annihilation into hadrons and a flux factor that depends on s and Q^2 only [2]:

$$\frac{{\rm d}\sigma}{{\rm d}Q^2} = \frac{4\alpha^3}{3sQ^2} R(Q^2) \left\{ \frac{(1+\frac{Q^4}{s^2})}{(1-\frac{Q^2}{s})} \log\frac{1+c_m}{1-c_m} - \left(1-\frac{Q^2}{s}\right) c_m \right\} , \quad (7)$$

and

$$R(Q^2) = \frac{\sigma(e^+e^- \to N\bar{N})}{\sigma_{\rm point}} = \frac{\beta_N}{2}\left(2|G_M^N|^2 + \frac{1}{\tau}|G_E^N|^2\right) , \quad (8)$$

where $c_m = \cos\theta_\gamma^{\rm min}$ and $\beta_N^2 = 1 - 4m_N^2/Q^2$.

After integration over the whole range of nucleon angles, the separation of electric and magnetic form factors is no longer feasible. However, the modulus of their ratio can be determined from the study of properly chosen angular distributions.

The close connection between this analysis and the one based on the reaction $e^+e^- \to N\bar{N}$ becomes apparent once the result is expressed in terms of the polar and azimuthal angles $\hat{\theta}$ and $\hat{\varphi}$, which characterize the nucleon direction in the rest frame of the hadronic system, with the z-axis opposite to the direction of the real photon momentum and the y-axis in the plane spanned by the beam and the photon direction. In the limit $Q^2 \ll s$

$$L_{\mu\nu}H^{\mu\nu} \approx \frac{(4\pi\alpha)^3}{Q^2}\frac{(1+\cos^2\theta_\gamma)}{(1-\cos^2\theta_\gamma)} \times 4\left(|G_M^N|^2(1+\cos^2\hat{\theta}) + \frac{1}{\tau}|G_E^N|^2\sin^2\hat{\theta}\right) . \quad (9)$$

(A more detailed discussion of angular distribution can be found in [15].) It is instructive to compare the angular distribution in Eq. (9) with the angular distribution from $e^+e^- \to N\bar{N}$:

$$\frac{d\sigma}{d\Omega} = \frac{\alpha^2\beta_N}{4Q^2}\left(|G_M^N|^2(1+\cos^2\theta) + \frac{1}{\tau}|G_E^N|^2\sin^2\theta\right) . \quad (10)$$

The close relation between Eqs. (9) and (10) is clearly visible.

As is already evident from the hadronic tensor in Eq. (6), the phases of the form factors are, however, not accessible by this method. Their determination would require the measurement of the polarization of the nucleons in the final state [16,17]. PHOKHARA can easily be extended to describe this additional degree of freedom. This option is of particular interest for $\Lambda\bar{\Lambda}$ production, with its self-analysing decay mode.

As will be discussed below, the event rate drops rapidly with increasing Q^2 and only few events will be observed for invariant hadron masses around 3 GeV. However, the rate for baryon pair production from J/ψ decays will be significantly enhanced, all considerations given above for continuum production do apply, and a precise measurement of the branching ratio of J/ψ into baryon pairs and the relative strength of magnetic and electric coupling is within reach.

Data giving information about the form factors in the time-like region originate from the reactions $e^+e^- \to p\bar{p}$ (and $p\bar{p} \to e^+e^-$) as shown in Fig. 2. The parametrization of the form factors used in PHOKHARA has been adopted from Ref. [18], and is described in detail in [15]. A free parameter, denoted θ is set to $\theta = \pi/4$ or $\theta = 19\pi/64$ as recommended in [12].

Only measurements of the total cross section are available. Form factors, if available at all, are extracted under the assumption $G_M^p = \mu_p G_E^p$, and no true separation of the electric and magnetic form factors has been performed. The poor experimental knowledge can be substantially improved by using the radiative return at B-meson factories and the separation of electric and magnetic form factors may be envisaged. The differential cross section as a function of Q^2, as observed through the radiative return, is shown in Fig. 3 for $p\bar{p}\gamma$. Similar results are obtained for $n\bar{n}\gamma$. The upper curve represents the cross section after integration over all proton angles and over photon angles down to 5° w.r.t. the beam direction. The lower curve is valid for cuts corre-

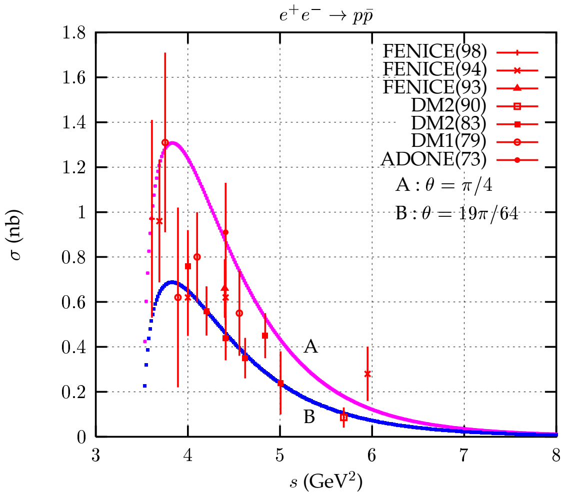

Figure 2. Comparison of the measured [19–25] $e^+e^- \to p\bar{p}$ cross section with the model from Ref.[18]. Predictions are given for two different values ($\pi/4$ - curve A and $19\pi/64$ - curve B) of the parameter θ.

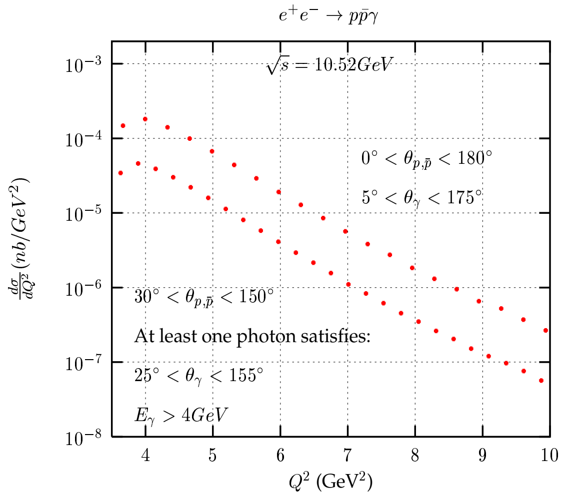

Figure 3. Differential cross section of the process $e^+e^- \to p\bar{p}\gamma(\gamma)$ for two different sets of cuts.

sponding to the BaBar acceptance region transformed to the e^+e^- cms. The event rates accumulated at B-factories already now, may be large enough to extract and separate $|G_M^N|$ and $|G_E^N|$. To explore the sensitivity to the form factors individually, we compare the differential cross sections obtained for the model described above with the distribution obtained under the assumption $G_M^p = \mu_p G_E^p$, subject, however, to the constraint that $\sigma(e^+e^- \to p\bar{p})$ (see Eq. (8)) remains unaffected. The angular distribution of the baryons, if defined in the laboratory or cms frame, is strongly affected by the boost. The difference between different choices for the form-factor ratios is expected to be more pronounced for the proton angular distribution in the hadronic rest frame, with the z-axis aligned with the direction of the photon and the y-axis in the plane spanned by the beam and the photon directions (see Eq.(9) above). For $Q^2 \ll s$, the case relevant to the present discussion, the pronounced dependence of the $\cos\hat{\theta}$ distribution on the choice of the form factors is clearly visible (Fig. 4).

The importance of the radiative corrections has been studied in [15]. The use of the NLO generator is highly recommended.

4. Pion and Kaon Form Factors at large Q^2

In the near future the experimental knowledge on the pion and kaon form factors $F_{\pi,K}(s)$ will be substantially improved, due to new data to be obtained using the radiative return method. The first measurements of F_π with this technique in the ρ region have already been performed by the KLOE Collaboration [26]. At larger energies, up to 2.0-2.5 GeV, perhaps even 3 GeV, accurate measurements of $F_{\pi,K}$ are anticipated from the BABAR experiment. The high rates expected at $s \gg m_\rho^2$ demand phenomenological models more elaborated than the simple ρ- (ρ, ω, ϕ-) dominance models for F_π (F_K). In [27] an ansatz was suggested that is valid in the region below at, and far above ρ-resonance and extended to the kaon form factor. It obeys the constraints from analyticity and isospin-symmetry and incorporates the proper behaviour at high energies, consistent with perturbative QCD, and the correct normalization at $s = 0$. Furthermore it is based on plausible assumptions derived from the quark model, moderate SU(3)-breaking, vector dominance and a pattern of radial excitations expected from dual resonance models.

Above the ρ-resonance the excited $\rho'(1450)$ and $\rho''(1700)$ are expected to play an important role. Already now these two states are indispensable, if

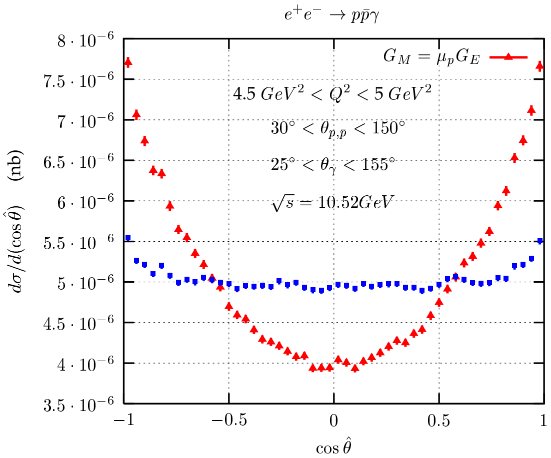

Figure 4. Angular distributions in the polar angle of the proton a typical different range of Q^2, with and without the constraint $G_M^p = \mu_p G_E^p$ (see text for a more detailed explanation).

one wants to accommodate the measured parameters of the ρ-resonance with the correct normalization of $F_\pi(s)$ at $s = 0$. In general, to include all possible intermediate hadronic states in the $\gamma^* \to \pi^+\pi^-$ transition amplitude, one has to take into account an infinite series of radially excited ρ's. In addition, there are multi-hadron intermediate states with $J^P = 1^-$ and $I = 1$ $(2\pi, 4\pi, K\bar{K}$ etc.). On the other hand, at sufficiently large s one expects $F_\pi(s) \sim \alpha_s(s)/s$, as predicted from perturbative QCD [28] for the pion form factor in the space-like region at $s \to -\infty$, analytically continued to $s \to +\infty$.

Models of hadronic amplitudes, where an infinite series of resonances at $s > 0$ is summed to yield a power-law behaviour at $s < 0$, are rooted in the Veneziano amplitude and dual resonance models formulated long before the advent of QCD. Recently, the model for the pion form factor using the masses and coefficients chosen according to Veneziano amplitude was considered in [29]. In [27] the dual-QCD$_{N_c=\infty}$ model was used as a starting point, modified for the first few ρ resonances, by keeping their parameters (masses, widths and coefficients) free and fitting them to experiment. In this way, the complicated effects of ρ resonances coupled to multi-hadron $(2\pi, 4\pi$ etc.) states were implicitly taken into account.

4.1. The pion form factor

The following model for the pion form factor has been adopted:

$$F_\pi(s) = \left[\sum_{n=0}^{3} c_n BW_n(s)\right]_{fit} + \left[\sum_{n=4}^{\infty} c_n BW_n(s)\right]_{dual-QCD_{N_c=\infty}}, \quad (11)$$

where in the ρ contribution $(n = 0)$ the $\rho - \omega$ mixing is included. The parameters of the four lowest $\rho_{0,1,2,3}$ states (i.e. $\rho, \rho'(1450)$, $\rho''(1700)$ and ρ''') are fitted to data and BW_n denotes a Breit-Wigner resonance amplitude.

Let us emphasize the main qualitative features of this model. It nicely matches the existing ρ-dominance models at $\sqrt{s} < 1$ GeV, simply because the $\rho_{n>2}$ states play a minor role in the $\sqrt{s} < 1$ GeV region. It is flexible, that is, it allows to vary the proportion of fitted and modeled resonances above ρ. E.g., with sufficiently precise data at higher energies one can include also the ρ_4-state into the 'fit' part. Alternatively, ρ_3 can be removed from the 'fit' part and added to the dual-QCD$_{N_c=\infty}$ part. Furthermore, as mentioned already, $F_\pi(s)$ as given above, can be easily continued to $s < 0$ and compared with the experimental data and QCD predictions in the space-like region. Accordingly, one gets a smooth power-like behaviour at asymptotically large time-like s.

We have fitted the model (11) to the existing data for the time-like pion form factor. The results of the fit for two different versions of BW-formulae (KS and GS for the first three resonances $\rho_{0,1,2}$), are plotted in Fig. 5. The most spectacular result of the fit is the change of the ρ'' coefficient c_2 with respect to the model [29] and to the earlier fits [30], from negative values $\sim -(0.02 - 0.04)$ to smaller but positive values $\sim$ 0.01-0.02. The positive sign is a direct consequence of the dip in the cross section around 1.6 GeV. Furthermore, the fitted mass of ρ' (1360-1380 MeV) gets shifted with respect to the PDG value (1465±25 MeV). The values of the masses and widths of ρ, ρ', ρ'' as well as c_0 and c_1 are in the ballpark of the dual-QCD$_{N_c=\infty}$ model. The

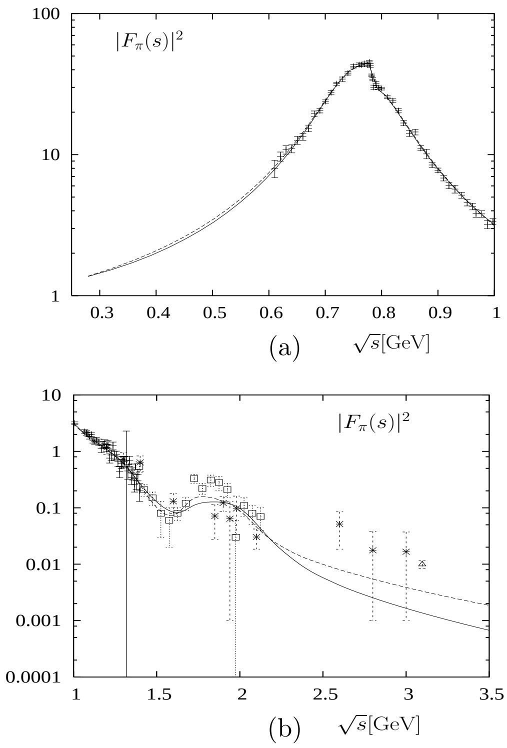

Figure 5. The pion form factor squared $|F_\pi(s)|^2$ as a function of $\sqrt{s}$ fitted to the data in the region near (a) and above (b) ρ resonance. The solid (dashed) line corresponds to the KS(GS) parameterization of BW formula.

same is true for the magnitude of c_2, its positive sign is enforced by the dip around 1.6 GeV and might be a consequence of the strong mixing between ρ'' and nearby resonances.

The data points with large errors at $\sqrt{s} = 2.5 \div 3$ GeV are systematically higher than the fitted curve, and the value of $F_\pi(\sqrt{s} = m_{J/\psi})$ extracted from the $J/\psi \to 2\pi$ partial width is larger than the model prediction by a factor of about three (this point was not included into the fit). For the time being it seems difficult to accommodate a pion form factor as large as the one derived from J/ψ decay.

To check our model further $F_\pi(s)$ was continued to $s < 0$ and successfully compared with the data there. Furthermore, reasonable agreement between the model and the QCD light-cone sum rule (LCSR) predictions [31,32] was observed.

4.2. Charged and neutral kaon e.m. form factors

The analogous strategy was adopted to describe the kaon form factors. Combining information on K^+K^- and $K^0\bar{K}^0$ production with constraints from isospin symmetry, and using assumptions deduced from the quark model and the OZI rule, it is possible to separate the $I = 1$ and $I = 0$ amplitudes in the form factor, and even the ω- and ϕ-components of the $I = 0$ part. The $I = 1$ part can then be used to predict the rate for $\tau \to \nu K^- K^0$. The ansatz for the kaon form factors adopted in [27] reads:

$$
\begin{aligned}
&F_{K^+/K^0}(s) = \\
&\pm\frac{1}{2}(c^K_\rho BW_\rho(s) + c^K_{\rho'} BW_{\rho'}(s) + c^K_{\rho''} BW_{\rho''}(s)) \\
&+\frac{1}{6}(c^K_\omega BW_\omega(s) + c^K_{\omega'} BW_{\omega'}(s) + c^K_{\omega''} BW_{\omega''}(s)) \\
&+\frac{1}{3}(c_\phi BW_\phi(s) + c_{\phi'} BW_{\phi'}(s)). \qquad (12)
\end{aligned}
$$

The resulting curves for the form factors are plotted in Fig. 6. Most importantly, fitting the kaon form factor above ϕ resonance, it is indeed possible to extract separate ρ, ω, ϕ components, which was not possible in the ϕ region due to the dominance of this resonance. Two different variants of the fit were carried out:

(1) the *constrained* fit (motivated by the quark model) where the normalization factors for ω resonances are fixed: $c^K_{\omega,\omega',\omega''} = c^K_{\rho,\rho',\rho''}$ and only the normalization factors for the ρ resonances are fitted (solid line);

(2) the *unconstrained* fit, where ω- and ρ- factors are fitted as independent parameters (dashed line).

We find the pattern of the normalization factors $c^K_{\rho,\rho'}$ for the first two ρ-resonance to be very similar to the corresponding values $c_{0,1}$ obtained in the pion form factor fits. These factors can be immediately translated into the strong couplings dividing out the decay constants of vector mesons. The latter are independently measured in the leptonic decays revealing a very mild SU(3) breaking, at the level of 10 %; according to the data

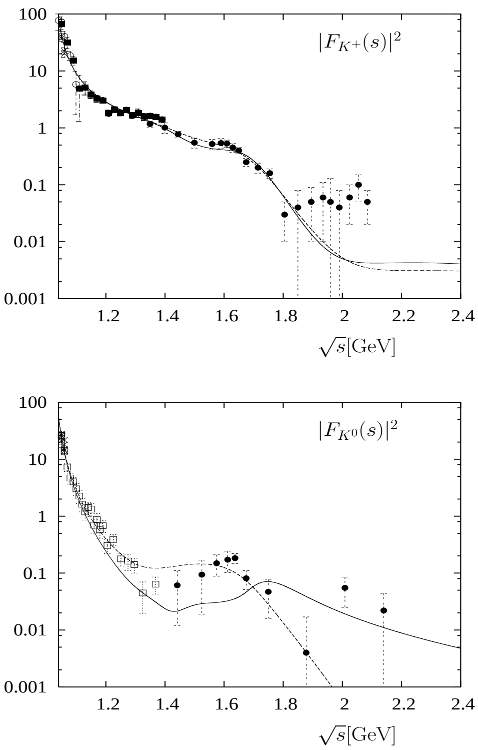

Figure 6. The charged and neutral kaon form factor squared as a function of $\sqrt{s}$ in the region above the ϕ resonance.

in [33]: $f_\rho \simeq 220$ MeV, $f_\omega \simeq 195$ MeV and $f_\phi \simeq 228$ MeV. The SU(3)-violating difference between the couplings of ρ and ϕ to kaons estimated from comparing c_ρ^K and c_ϕ is also moderate in both versions of the fit.

4.3. Predicting $\tau \to K^- K^0 \nu_\tau$ decay distribution and rate

The isospin one part of the e.m. kaon form factor, can be used to predict the $\tau \to K^- K^0 \nu_\tau$ decay width. The fitted values for $c^K_{\rho,\rho',\rho''}$ from e^+e^- annihilation thus allow to calculate the decay rate and distribution. The normalized distribution is plotted in Fig.7 and (qualitatively) compared with the event distribution in the kaon pair mass, measured by CLEO Collaboration [34,35]. The branching ratio prediction for the $BR(\tau \to K^- K^0 \nu_\tau) = 0.19 \pm 0.01\%$ $(0.13 \pm 0.01\%)$ for the constrained (unconstrained) fit can be compared with the experimentally measured value [33] $BR(\tau \to K^- K^0 \nu_\tau) = 0.154 \pm 0.016\%$. Both the decay distribution and the decay width are very sensitive to the pattern of ρ resonances in the isospin-1 form factor. Generally, the width grows with increasing contributions from the excited ρ-mesons, an effect observed earlier in [36].

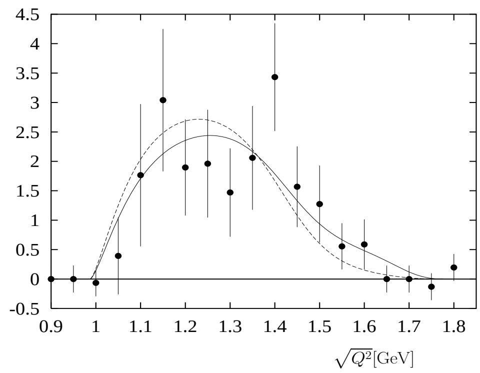

Figure 7. Normalized distribution in the kaon pair invariant mass $\sqrt{Q^2}$ obtained from the fitted kaon form factor; the solid (dashed) line corresponds to the constrained (unconstrained) fit.

Acknowledgements

This contribution is based on work performed in collaboration with C. Bruch, H. Czyż, A. Grzelińska, A. Khodjamirian and G. Rodrigo. I would like to thank A. Denig, W. Kluge, and S. Müller for discussion of experimental aspects and A. Grzelińska for help with the preparation of the manuscript.

REFERENCES

1. K. G. Chetyrkin, J. H. Kühn and A. Kwiatkowski, Phys. Rep. **277** (1996) 189; R. V. Harlander and M. Steinhauser, Comput. Phys. Commun. **153** (2003) 244 [hep-ph/0212294].
2. S. Binner, J. H. Kühn and K. Melnikov, Phys. Lett. B **459** (1999) 279 [hep-ph/9902399].
3. Min-Shih Chen and P. M. Zerwas, Phys. Rev. D **11** (1975) 58.

4. H. Czyż and J. H. Kühn, Eur. Phys. J. C **18** (2001) 497 [hep-ph/0008262].
5. G. Rodrigo, A. Gehrmann-De Ridder, M. Guilleaume and J. H. Kühn, Eur. Phys. J. C **22** (2001) 81 [hep-ph/0106132].
6. G. Rodrigo, H. Czyż, J.H. Kühn and M. Szopa, Eur. Phys. J. C **24** (2002) 71 [hep-ph/0112184].
7. J. H. Kühn and G. Rodrigo, Eur. Phys. J. C **25** (2002) 215 [hep-ph/0204283].
8. H. Czyż, A. Grzelińska, J. H. Kühn and G. Rodrigo, Eur. Phys. J. C **27** (2003) 563 [hep-ph/0212225].
9. in preparation
10. G. Cataldi, A. Denig, W. Kluge, S. Muller and G. Venanzoni, Frascati Physics Series (2000) 569; A. Denig *et al.* [KLOE Collaboration], eConf **C010430** (2001) T07 [hep-ex/0106100], Nucl. Phys. Proc. Suppl. 116 (2003)243 [hep-ex/0211024]; A. Aloisio *et al.* [KLOE Collaboration], hep-ex/0107023; E. P. Solodov [BABAR collaboration], eConf **C010430** (2001) T03 [hep-ex/0107027].
11. H. Czyż, A. Grzelińska, J. H. Kühn and G. Rodrigo, Eur. Phys. J. **C83** (2004) 333, [hep-ph/0308312].
12. F. Iachello, nucl-th/0312074 and talk at Workshop on e^+e^- in the 1–2 GeV range: Physics and Accelerator Prospects, Alghero, Sardinia (Italy), 10-13 September, 2003.
13. S. J. Brodsky, C. E. Carlson, J. R. Hiller and D. S. Hwang, [hep-ph/0310277]
14. Baldini, R. *et al.*, eConf **C010430** (2001) T20 [hep-ph/0106006]; Eur. Phys. J. **C11** (1999) 709.
15. H. Czyż, J.H. Kühn, E. Nowak and G. Rodrigo, Eur. Phys. J. **C35** (2004) 527, [hep-ph/0403062].
16. A. Z. Dubnickova, S. Dubnicka and M. P. Rekalo, Nuovo Cim. **A109** (1996) 241.
17. S. Rock, eConf **C010430** (2001) W14 [hep-ex/0106084].
18. F. Iachello, A. D. Jackson and A. Lande, Phys. Lett. **B 43** (1973) 191.
19. A. Antonelli *et al.* (FENICE collaboration), Nucl. Phys. **B517** (1998) 3.
20. A. Antonelli *et al.* (FENICE collaboration), Phys. Lett. **B 334** (1994) 431.
21. A. Antonelli *et al.* (FENICE collaboration), Phys. Lett. **B 313** (1993) 283.
22. D. Bisello *et al.* (DM2 collaboration), Z. Phys. **C48** (1990) 23.
23. D. Bisello *et al.* (DM2 collaboration), Nucl. Phys. **B224** (1983) 379.
24. B. Delcourt *et al.* (DM1 collaboration), Phys. Lett. **B 86** (1979) 395.
25. M. Castellano *et al.* (ADONE collaboration), Nouvo Cim. **14A** (1973) 1.
26. A. Aloisio *et al.* [KLOE Collaboration], arXiv:hep-ex/0312056.
27. C. Bruch, A. Khodjamirian and J.H. Kúhn, hep-ph/0409080.
28. G. P. Lepage and S. J. Brodsky, Phys. Lett. **87B** (1979) 359; Phys. Rev. **D22** (1980) 2157; A. V. Efremov and A. V. Radyushkin, Phys. Lett. **B94** (1980) 245; Theor. Math. Phys. **42** (1980) 97;
V. L. Chernyak and A. R. Zhitnitsky, JETP Lett. **25** (1977) 510; Sov. J. Nucl. Phys. **31** (1980) 544;
G. R. Farrar and D. R. Jackson, Phys. Rev. Lett. **43** (1979) 246.
29. C. A. Dominguez, Phys. Lett. B **512** (2001) 331.
30. J. H. Kühn and A. Santamaria, Z. Phys. C **48** (1990) 445.
31. V. M. Braun and I. E. Halperin, Phys. Lett. B **328**, 457 (1994);
V. M. Braun, A. Khodjamirian and M. Maul, Phys. Rev. D **61**, 073004 (2000).
32. J. Bijnens and A. Khodjamirian, Eur. Phys. J. C **26** (2002) 67.
33. S. Eidelman *et al.* [Particle Data Group Collaboration], Phys. Lett. B **592** (2004) 1.
34. T. E. Coan *et al.* [CLEO Collaboration], Phys. Rev. D **53** (1996) 6037.
35. R. Barate *et al.* [ALEPH Collaboration], Eur. Phys. J. C **4** (1998) 29.
36. M. Finkemeier, J. H. Kühn and E. Mirkes, Nucl. Phys. Proc. Suppl. **55C**, 169 (1997).